2022

Transient Analysis Of Startup Characteristics Of A Water-lubricated Twin-screw Air Compressor System

Yishuang Liu

Chuang Wang

Xinzhong Liao

Ziwen Xing

Transient analysis of startup characteristics of a water-lubricated twin-screw air compressor system

Yishuang Liu, Chuang Wang*, Xinzhong Liao, Ziwen Xing

School of Energy and Power Engineering, Xi'an Jiaotong University,
Xi'an, Shaanxi, PR China

* Corresponding Author. E-mail: chuangwang@xjtu.edu.cn

ABSTRACT

Water-lubricated twin-screw compressors have attracted wide attention because they can supply oil-free compressed air at an acceptable cost. However, the injection of water as auxiliary fluid for lubrication could result in different transient characteristics of the compressor and system during the starting period due to the poor lubricity of water. For the purpose of clarifying the startup characteristics and thus increasing the performance and reliability of the water-lubricated twin-screw air compressor, the simulation and corresponding experiments are implemented on a water-lubricated screw air compressor system to study variations of water injection parameters and pressure distribution during the startup condition. The thermodynamic model of the whole system including compressor, water cooler, water-gas separator and water pump is established using MATLAB/Simulink and is verified by the experimental results with enough accuracy. Based on the verified dynamic model, a control method is proposed to ensure that the air compressor system runs reliably during the startup stage. The energy-saving potential and reliability of the startup control method are evaluated experimentally, which demonstrated its feasibility used in the water-lubricated twin-screw air compressor system.

1. INTRODUCTION

With the rapid development of the national economy, the safety and health of the pharmacy and food processing industry have drawn lots of attention. Compressed air is one of the essential power sources for modern industries. Therefore, it is important and necessary to reduce the contamination of compressed air for the quality of medicine and food. Oil-injected twin-screw compressors are widely used in the industry to produce compressed air with the advantages of high reliability, high efficiency, well-adapted, easy operation and low maintenance cost[1]. Compared to conventional oil-free compressors, the injection of oil can improve the efficiency and reliability of compressors significantly[2]. However, the oil used in the compressors cannot be completely separated from the compressed air, which means the compressed air is polluted. As one kind of oil-free twin-screw compressor, the water-lubricated twin-screw compressors using water as the lubricant could prevent compressed air from oil contamination thoroughly[3].
Injecting water into screw compressors has been proposed for a long time to replace dry screw compressors due to the advantages of improving efficiency and lowering the gas temperature. Stosic *et al*.(2004) confirmed that injecting volatile fluid will lower discharge temperature through experiments several years ago[4]. Tian *et al*.(2017) established a mathematical model for a water-injected twin-screw water vapor compressor by taking heat and mass transfer between working fluid and injected water into consideration[5]. Yang *et al*.(2018) established a test rig for a water-injected process-gas screw compressor and studied the effects of different parameters on performance characteristics by experiments[6]. Wang *et al*.(2018) developed a prototype of the water-lubricated twin-screw compressors and investigated the influences of different operating parameters through experiments[7]. Wang also studied the characteristics of a water-lubricated twin-screw compressor system from perspectives of wear, leakage and bearing[8-10].
However, the research above focuses on the steady-state characteristics of the water-injected or water-lubricated twin-screw compressor system. During startup period, parameters in compressor systems such as temperature and pressure change rapidly, which makes the system unstable and hard to control. Hence, investigating startup characteristics is necessary and urged. Some researchers have reported their investigations on startup characteristics under different parameters of twin-screw compressors. Krichel *et al*.(2010) built a dynamic model for an oil-flooded twin helical screw compressor, which contains four stages: warm-up, idle, full load and shut-down. Validated by experiments, this

model improved the control strategies and reduced energy losses of compressor stations[11]. Chukanova *et al*.(2012) investigated the oil-flooded twin-screw compressors startup process with different initial discharge pressure by experiments[12]. Polo *et al*.(2017) established a dynamic model by Simulink composed of a control valve with its PID control loop, separator, heat exchanger and screw compressor[13]. Some studies about startup characteristics of other kinds of compressors are also reported. Link *et al*.(2011) proposed a comprehensive mathematical model of the reciprocating compressor to predict piston motion, pressure in the compression chamber and valve displacement with the experimental verification[14]. Wu *et al*.(2017) studied the warm startup characteristics of a rotary compressor through experiments and compared results with cold startup characteristics[15]. Zhu *et al*.(2020) used a visualization technique to analyze the oil climbing process of a rolling rotary compressor during the startup period[16]. Arqam *et al*. (2021) derived and verified a transient swash-plate compressor model to clarify the effects of inertia, line pressures, viscous losses and bearing resistance on startup torque[17]. Zhou *et al*. (2021) build a simulation model by Labview to study the effect of ambient temperature and power frequency on linear compressors startup characteristics[18]. From the literature above, researches on the startup characteristics of water-lubricated compressors have not been presented yet. The low viscosity of water leads to the poor lubricity compared to the oil, which causes the different startup characteristics between systems using oil and water. To avoid dry friction of water-lubricated journal bearings, the startup characteristics of the water-lubricated twin-screw air compressor system need to be investigated and evaluated carefully.

This paper establishes a dynamic model of a water-lubricated twin-screw air compressor system with an intelligent control method. The process of pressure establishment, the variation of water mass flow and the water-gas ratio are calculated to study the startup characteristics of this system. The accuracy of this model is verified experimentally. Based on the dynamic model, the effects of different rotation speeds, discharge pressure and pump types on the system performance during the startup period are investigated and the control method is improved to be more suitable for real compressor systems.

2. MODEL OF COMPRESSOR SYSTEM

The model is composed of the main components of a water-lubricated twin-screw air compressor system: compressor, water-gas separator, valves, water cooler, pump and pipes. The principle of constructing components will be discussed in subsections.

The available control mothed is by setting time to open compressor and close water pump. This setting time is usually set by experience. However, the setting time is not suitable for different operating parameters. The model adopts an intelligent control method. The control method includes two steps. First, the water pump starts to provide a certain amount of water to prevent dry friction. The amount of water is calculated by the volume of the bearing chamber and rotor chamber, in this system the amount of water is 0.51kg. Second, the pump is turned off as the water-gas ratio without the pump reaches a setting point, 13.5 in this system, which means enough water flows into the compressor.

For the real system control method, water mass and water-gas ratio in the compressor are difficult to measure. Therefore, the setting point of water mass could be replaced by a setting time for the real system control method, setting point of water-gas ratio could be replaced by a setting point of water injection pressure. The values of the two setting points are calculated by simulation.

2.1 Assumption

To simplify the model, three assumptions are employed in the total system:

(1) Neglecting the hysteresis of pressure change caused by flow velocity.

(2) Neglecting the compressor thermal inertia.

(3) Neglecting the pulsation of water and air in the subsections.

2.2 Compressor

Due to the water used for lubrication, air, water and steam are involved in the working process of the compressor simultaneously.

The calculation equation of the mass flow rate of dry air can be obtained by the following:

$$q_{\mathrm{m,a}} = \frac{\eta_{\mathrm{v}} q_{\mathrm{Vt}}}{v_{\mathrm{in}}} \tag{1}$$

where n is the rotation speed, and η_v is the volumetric efficiency. With the profile of increasing motor speed, the variation of mass flow rate during the startup period can be described.

The calculation equation of shaft power can be obtained by the following:

$$P_{\text{shaft}}=\frac{\left(h_{\text{s,out}}\text{-}h_{\text{in}}\right)}{\eta_{\text{ad}}}q_{\text{m,a}} \tag{2}$$

where η_{ad} is the adiabatic efficiency. The data of two efficiencies is provided by previous experiments of literature [7]. The thermal equilibrium by the following is used to obtain discharge temperature:

$$P_{\text{shaft}}=q_{\text{m,a}}\left(h_{\text{out,a}}\text{-}h_{\text{in,a}}\right)+q_{\text{m,w,in}}\left(h_{\text{out,w}}\text{-}h_{\text{in,w}}\right)+q_{\text{m,v,in}}\left(h_{\text{out,v}}\text{-}h_{\text{in,v}}\right)+q_{\text{m,ex}}\left(h_{\text{out,v}}\text{-}h_{\text{out,w}}\right) \tag{3}$$

2.3 Water pump

The pump used in the experiment is a DS-360 roller vane pump. By the data provided by the manufacturer, the characteristic curve is fitted as Eq (4) for the model. Flow in the pump is assumed as an isothermal process.

$$Q=-0.05035\Delta p+6.029 \tag{4}$$

where ΔP is the pressure difference between the inlet and outlet, Q is the volumetric flow rate.
For comparison, one centrifugal pump of similar motor power, whose type is MY-2-6000-MK, is used in the model. The characteristic curve provided by the same manufacturer is fitted as Eq (5).

$$H=-0.0171Q\text{^}2+0.0827Q+14.774 \tag{5}$$

where H is the total head.

2.4 Method to calculate the mass flow rate of injection water

The water flow is driven by the pump or pressure difference. Therefore, figuring out the pressure loss of each component and the pressure difference between the compressor and water-gas separator is the key to calculating the water flow rate. The pressure loss model consists of pipes, valves and a water cooler.
The pressure loss of pipes and water cooler are calculated by the Darcy-Weisbach formula shown in Eq (6).

$$\begin{cases} H_{\text{f}}=\lambda\dfrac{L}{D}\dfrac{v^2}{2g} \\ H_{\text{l}}=\alpha\dfrac{v^2}{2g} \end{cases} \tag{6}$$

where λ is friction coefficient, α is local resistance coefficient, H_{f} is the friction loss of head, and H_{l} is the local resistance loss of head.
The Moody chart is fitted as Eq (7) to calculate the friction coefficient.

$$\begin{cases} \lambda=\dfrac{0.3164}{Re^{0.25}} & Re<1e5 \\ \lambda=0.032+\dfrac{0.221}{Re^{0.237}} & Re>1e5 \end{cases} \tag{7}$$

The pressure loss of valves including the check valve is calculated by Bernoulli's equation.

$$q_{\text{m}}=AC_{\text{P}}\sqrt{2\rho\Delta p} \tag{8}$$

where C_P is flow coefficient, ρ is density.
Using empirical formula Eq (9) to calculate C_{P}.

$$C_{\text{P}}=0.02005\sqrt{\rho}+0.634v \tag{9}$$

where v is kinematic viscosity.

2.5 Description of the simulation model

Fig. 1 displays the schematic diagram of the entire model developed by MATLAB/Simulink. The components discussed above form the subsystems. The environment is used to provide ambient parameters. The pressure drop of the inlet filter is given by experiments, the value of which is 10kPa.

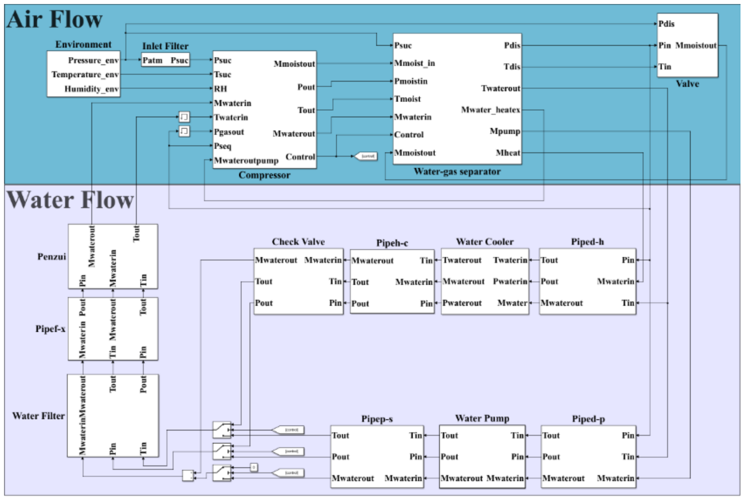

Fig. 1. Model of the water-lubricated twin-screw air compressor system

3. EXPERIMENTAL SETUP

To validate the accuracy of the mathematical model, a test tig is established to measure startup characteristics of the water-lubricated air compressor system.

3.1 Description of the test system

As shown in Fig. 2, the test system consists of an air filter, a water filter, a compressor, a water-gas separator, a water pump, a water cooler and the data measuring system. The system includes air flow and water flow. The inlet air is filtered by an inlet filter, then compressed in the chamber of the compressor and cooled by water. Subsequently, the mixture of air and water is discharged into the water-gas separator. Through gravity, centrifugal force and filter, water and air are separated. Flowing through a valve and a nozzle flowmeter to measure mass flow rate, the air is discharged into the atmosphere. The water pump is opened before the compressor startup to ensure enough water for lubrication and runs till there is enough pressure difference between the separator and compressor. Then the water is cooled by the fined tube water cooler. Afterward, the water flow is filtered by a water filter to reduce inclusion in the water. After flowing through the turbine flowmeter, the water is injected into the compressor chamber for lubrication and cooling, then discharged with compressed air into the water-gas separator. The rotation speed of the fan and motor are controlled by two frequency converters separately. Hence, the temperature of injected water is easy to regulate.

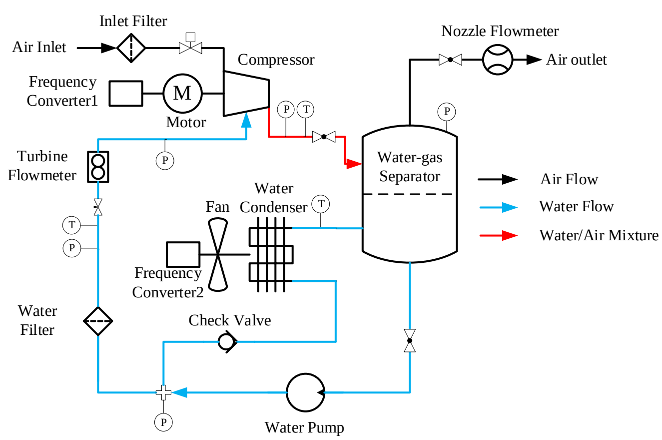

Fig. 2. Schematic diagram of the experimental system

Fig. 3 displays the complete system except for the data collector and power supply. Some components are connected by thread for the durability of connection and some components are connected by transparent flexible tubes for convenient installation. Two frequency converters are placed in the cabinet next to the power control cabinet. Due to the limitation of space, the data collector is placed at a distance connected to the system by signal lines.

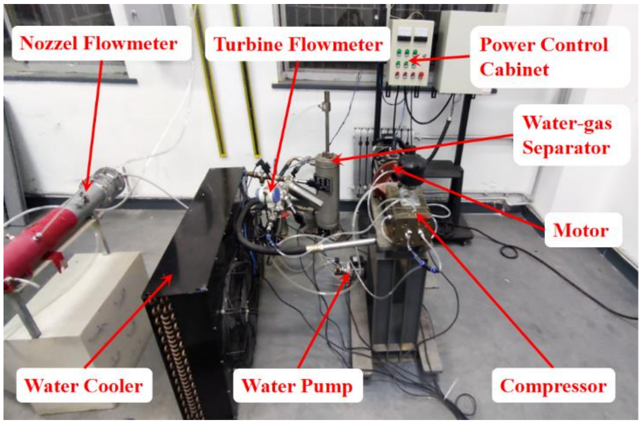

Fig. 3. Sketch of the experimental system components

3.2 Parameters of the data measuring system

In total, the data measuring system shown in Fig. 2 and Fig. 3 consists of 4 pressure sensors, 3 temperature sensors, a nozzle flowmeter, a turbine flowmeter, and a pressure gauge. The pressures of this system except the discharge pressure are measured by pressure sensors. The pressure sensors are YM-131, the measurement range is 0-2.5MPa, and the measurement accuracy is 0.5%. The temperature sensors are PCT200 with a measurement range of 0-100℃ and measurement accuracy of 0.5%. With the 0.25% measurement accuracy, the ASME nozzle flow meter is used to measure the volumetric flow rate. The water injection flow rate is measured by the EA-LWGY-15A turbine flow meter with a measurement range of 0.4-8m^3/h and a measurement accuracy of 0.5%. Agilent 34970A is the data collector with a collection accuracy of 0.02%. By the data measuring system, time-varying performance parameters are measured and collected. Ambient temperature and relative humidity are measured by a digital thermometer with the measurement precision of ±0.3℃ and ±3%RH. The ambient pressure is measured by a dial barometer aneroid barometer with a measurement precision of ±0.2kPa. Sensors and the turbine flow meter are powered by one 24V DC power supply.

4. RESULTS AND DISCUSSIONS

4.1 Validation of simulation model

To validate the mathematical model accuracy, one experiment is carried out under the rotation speed of 1800rpm and the discharge pressure of 5.2bar. Fig. 4 shows the comparison of simulated and experimental discharge pressure, pressure before water filter and pressure after water filter. The pressure increases slowly at the beginning, rises at a stabilizing speed and reaches stability in around 25 seconds. As shown in Fig. 4, the value and trend of simulation results are consistent with the experimental results. The time average error of discharge pressure is 2.52%. The time average errors of pressure before and after the water filter are 2.85% and 4.47%, respectively. The simulation model is proved accurate and effective to analyze the transient analysis of startup characteristics.

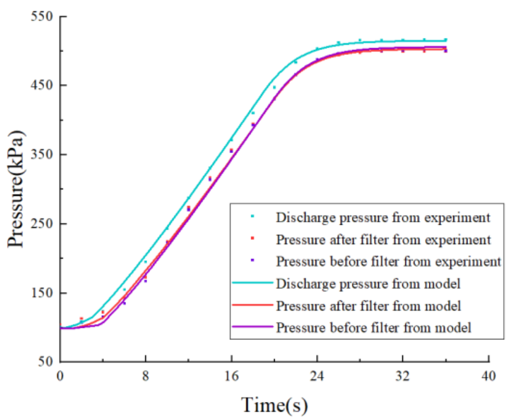

Fig. 4. Comparison of experiment and simulation on pressure distribution

4.2 Effect of rotation speed

Fig. 5 and Fig 6 show the time-varying flow rate, discharge pressure, injection pressure and water-gas ratio at rotation speeds of 3600rpm, 4800rpm and 6000rpm, the data below is the same order, under the discharge pressure of 7bar. The dashed line in Fig 6(b) is the setting value of water-gas ratio. It can be seen that the water flow rate, discharge pressure and injection pressure at different speeds are the same before 5.4s for the compressor is off. The water flow rate starts to increase at 7.5, 6.9s and 6.6s when pressure difference drives water to flow through the water cooler. The turning points at 9.6s, 10.5s and 12.6s with the triangle marks are the moment that the water pump is turned off due to the water-gas ratio reaching the setting point. The injection pressure decreases 24.25kPa, 27.30kPa and 47.61kPa without the pump. The increasing pressure drop is caused by the characteristic curve of roller vane pump. After the pressure is established, the operating characteristics keep to a steady state. The volumetric flow rate depending on rotation speeds influences the pressure establishment time, which is 25.8s, 20.4s and 17.1s. The effect of rotational speeds on the pressure establishment time becomes limited with the increase of rotational speed. The trend of injection pressure, water flow rate and other parameters are similar to the discharge pressure. Volumetric flow rate has a greater impact on water-gas ratio, by Fig. 6(b), the water-gas ratio with pump is 25.69, 18.31 and 14.19 after discharge pressure establishes. Hence, for high rotation speeds, the water-gas ratio decreases obviously which reduces reliability of the water-lubricated air compressor system.

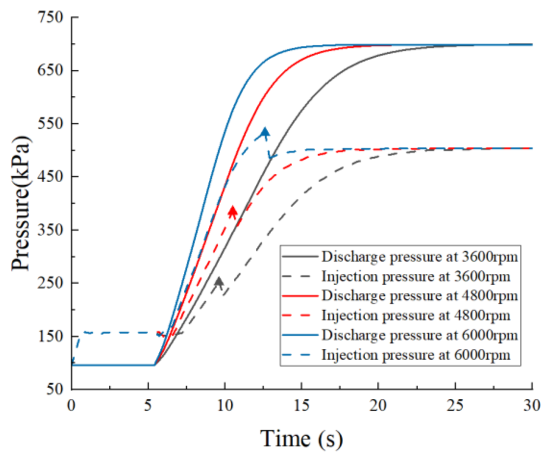

Fig. 5. Effect of rotation speed on pressure establishment

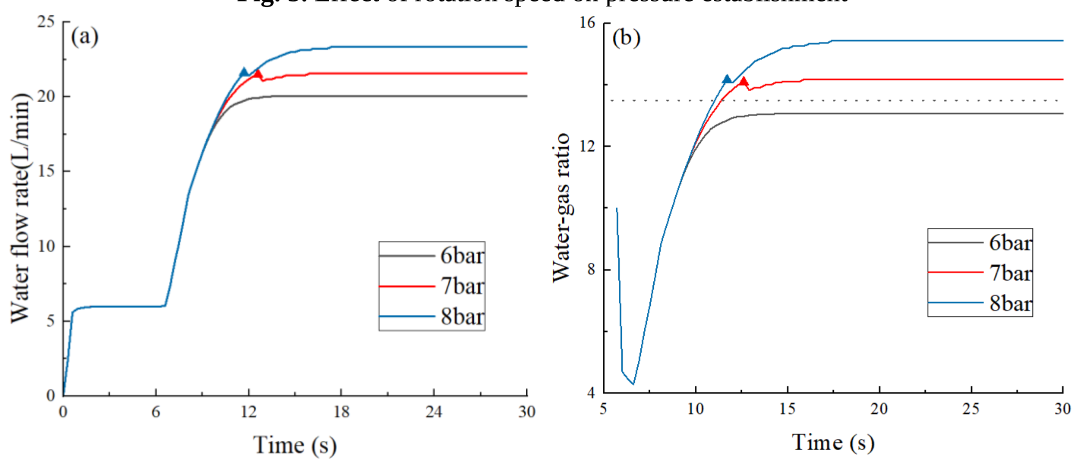

Fig. 6. Effect of rotation speed on flow rate water-gas ratio

4.3 Effect of setting discharge pressure

Fig. 7 and Fig. 8 show the influence of setting discharge pressure on water flow rate, injection pressure and the water-gas ratio at rotation speeds of 6000rpm under the setting discharge pressure of 6bar, 7bar and 8bar. The dashed line in Fig 8(b) is the setting value of water-gas ratio. The setting discharge pressure is controlled by a variable opening valve. Before the valve reaches minimum opening pressure until opens at 9.6s, there is no difference between the three discharge pressures. Due to the different valve openings, the pressure establishment time is 14.1s at 6bar, 17.4s at 7bar and 19.2s at 8bar. The effect of the discharge pressure on the pressure establishment process is less than the rotation speed. With the discharge pressure increasing, the water flow rate and the water-gas ratio increase. As shown in Fig. 8(b), the water-gas ratio with the pump at the setting discharge pressure of 6bar is below setting point 13.5, which means the system is operating without enough water. Low discharge pressure under 7bar at 6000rpm cannot provide enough water flow rate. Therefore, the water-lubricated air compressor system run under a low setting discharge pressure decreasing the system water-gas ratio, which decreases the reliability of the system.

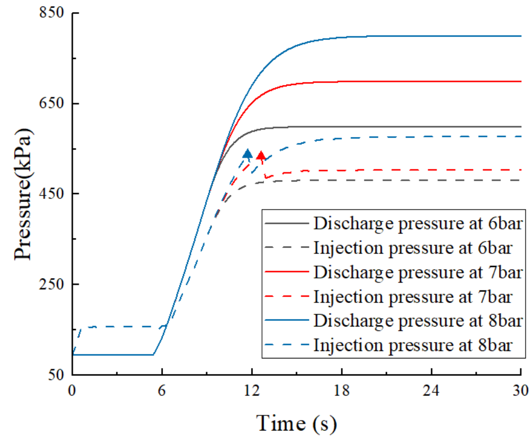

Fig. 7. Effect of setting discharge pressure on pressure establishment

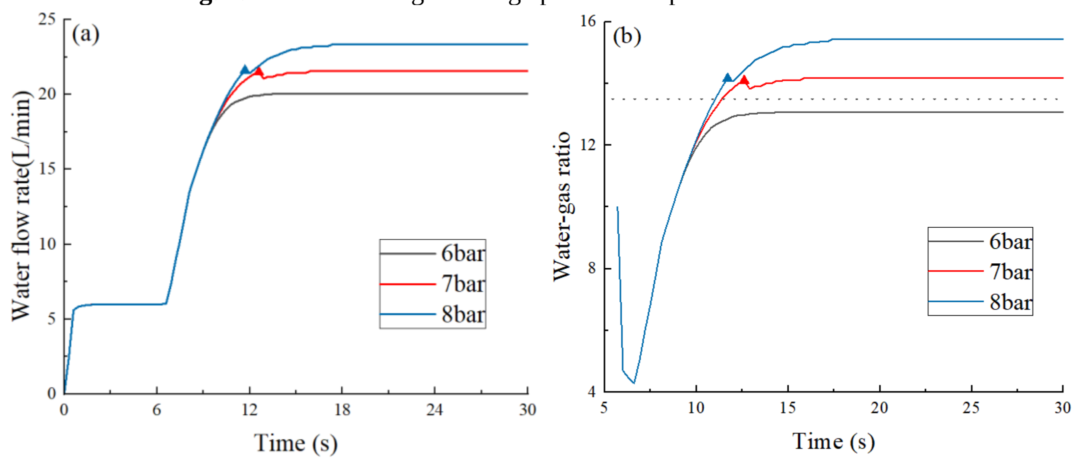

Fig. 8. Effect of setting discharge pressure on flow rate and water-gas ratio

4.4 Effect of pump type

Fig. 9 shows the influence on water flow rate and pressure of different types of pumps under the discharge pressure of 8bar and rotation speeds of 3600rpm and 4800rpm. The differences in the startup characteristics between the two pumps are the compressor starting time and pressure drop at the point the pump turns down. As shown in Fig .9(c), the water flow rate of roller vane pump reaches 6L/min at the very beginning due to the displacement principle. Hence, the system with roller vane pump starts 0.9 quicker than the system with centrifugal pump. Table 1 displays the pressure drop at the turning point. With the rotation speeds increasing, the roller vane pump maintains a high injection pressure and the centrifugal pump cannot provide a stable pressure rise. Therefore, the roller vane pump can increase more water flow rate and improve stability with similar energy consumption as discharge pressure increases.

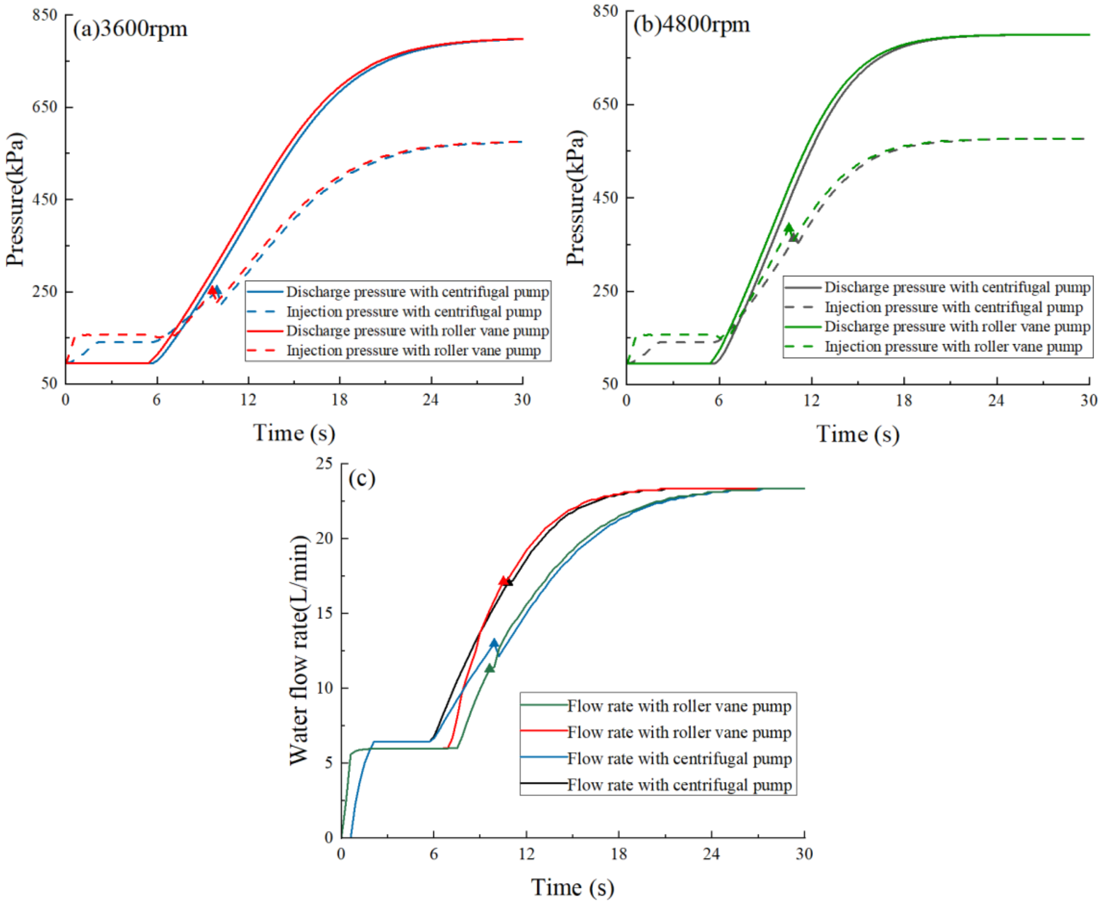

Fig. 9. Effect of pump type on water flow rate and pressure establishment

Table 1: Pressure drop at the point the pump turns down

Pump type	**Pressure drop at 3600 rpm(kPa)**	**Pressure drop at 4800 rpm(kPa)**	**Difference between 3600 rpm and 4800 rpm**
Centrifugal pump	28.26	9.92	-18.34
Roller vane pump	24.64	26.39	1.75

4.5 Values of real system setting point

In this simulation model, the setting parameters of starting the compressor and turning down the water pump are water mass in the compressor and water-gas ratio. The two parameters are not easy to measure, as section 2 discussed. For the convenience of real system control, Table 2 shows the setting parameters for turning down the water pump of the real compressor system. By simulation, 5.4s is the setting time for turning on the compress under this type of water pump. Through the control parameters calculated by simulation, the stability and intelligence of the compressor system startup process are improved and optimized.

Table 2: Value for the real system setting parameters

Rotation speeds(rpm)	3600	4800	6000
Injection pressure(kPa)	252.13	385.29	533.49

5. CONCLUSION

This paper constructs a mathematical model of a water-lubricated twin-screw air compressor system by MATLAB/Simulink and proposes a startup control method. This model takes the compressor, water pump, water-gas separator, water cooler, filters, pipes and valves into account and the result is verified by experiment. Using the proposed model, transient characteristics during the startup period of this system are calculated. The values of the real system setting point are calculated by the simulation model for stable and intelligent control. The following conclusions are obtained:

(1) The rotation speeds and setting discharge pressure influence pressure, water flow rate and water-gas ratio. Because the volumetric flow varies with rotation speeds. Increasing setting discharge pressure and decreasing rotation speeds can raise the water-gas ratio, which increases the reliability of the water-lubricated air compressor system.

(2) Compare to centrifugal pumps with similar motor power, the roller vane pump can provide stable water flow due to the displacement principle. For the same reason, the roller vane pump keeps a stable water head increment with the discharge pressure increases.

NOMENCLATURE

q_m	mass flow rate	kg/s
q_{Vt}	theoretical volumetric flow rate	m^3/s
q_V	volumetric flow rate	m^3/s
η	efficiency	
n	rotation speed	rpm
υ	velocity	m/s
	specific volume	m^3/kg
h	specific enthalpy	J/kg
P	power	kW
p	pressure	bar
Q	volumetric flow rate	L/min
H	head	m
L	length	m
D	diameter	m
g	gravitational acceleration	m/s^2
Re	Reynolds number	
A	area	m^2
ρ	density	kg/m^3

Subscript

υ	volumetric
ad	adiabatic
s	isentropic
out	outlet
in	inlet
a	dry air
w	liquid water
v	vapor
ex	exchange amount of liquid water and vapor

REFERENCES

1.Ziwen, X. (2000). Screw compressor-Theory, design and application. *China Machine Press*, 71-78.
2.Abdan, S., Basha, N., Kovacevic, A., Stosic, N., Birari, A., & Asati, N. (2019, August). Development and Design of Energy Efficient Oil-Flooded Screw Compressors. *In IOP Conference Series: Materials Science and Engineering* (Vol. 604, No. 1, p. 012015). IOP Publishing.

3.Madhav, K. V., & Kovačević, A. (2015, July). Economics of water injected air screw compressor systems. *In IOP Conference Series: Materials Science and Engineering* (Vol. 90, No. 1, p. 012012). IOP Publishing.
4.Stosic, N., Smith, I. K., & Kovacevic, A. (2004, January). Estimation and control of heat transfer in screw compressor rotors. *In ASME International Mechanical Engineering Congress and Exposition* (Vol. 47012, pp. 441-446).
5.Tian, Y., Shen, J., Wang, C., Xing, Z., & Wang, X. (2017). Modeling and performance study of a water-injected twin-screw water vapor compressor. *International Journal of Refrigeration*, 83, 75-87.
6.Yang, Q., Liu, C., Zhang, Q., Liu, G., Zhao, Y., & Li, L. (2018). Experimental investigation of the water–injected process-gas screw compressor. *Proceedings of the Institution of Mechanical Engineers, Part E: Journal of Process Mechanical Engineering*, 232(1), 3-11.
7.Wang, C., Xing, Z., Chen, W., Yang, Q., & He, Z. (2018). Development of an oil free water-lubricated twin-screw air compressor. *Applied Thermal Engineering*, 143, 396-402.
8.Wang, C., Xing, Z., Chen, W., Sun, S., & He, Z. (2019). Analysis of the leakage in a water-lubricated twin-screw air compressor. *Applied Thermal Engineering*, 155, 217-225.
9.Wang, C., Xing, Z., Pan, X., & He, Z. (2018). Simulation of the characteristics of the water-lubricated journal bearing in twin-screw air compressor. *Industrial Lubrication and Tribology*.
10.Wang, C., Xing, Z., Sun, S., Chen, W., & He, Z. (2021). Theoretical research on the wear characteristics of rotors in a twin-screw compressor. *Proceedings of the Institution of Mechanical Engineers, Part E: Journal of Process Mechanical Engineering*, 09544089211043612.
11.Krichel, S. V., & Sawodny, O. (2011). Dynamic modeling of compressors illustrated by an oil-flooded twin helical screw compressor. *Mechatronics*, *21*(1), 77-84.
12.Chukanova, E., Stosic, N., Kovacevic, A., & Dhunput, A. (2012). Investigation of Start Up Process in Oil Flooded Twin Screw Compressors.
13.Poli, G. W., Milligan, W. J., & McKenna, P. (2017, August). Dynamic modelling and PID loop control of an oil-injected screw compressor package. *In IOP Conference Series: Materials Science and Engineering* (Vol. 232, No. 1, p. 012066). IOP Publishing.
14.Link, R., & Deschamps, C. J. (2011). Numerical modeling of startup and shutdown transients in reciprocating compressors. *International Journal of Refrigeration*, 34(6), 1398-1414.
15.Wu, J., Lin, J., Zhang, Z., Chen, Z., Xie, J., & Lu, J. (2017). Experimental investigation of dynamic characteristics of a rotary compressor and its air conditioner using R290 during warm startup. *Applied Thermal Engineering*, 125, 1469-1477.
16. Zhu, Y., He, G., Sun, W., Shimoji, M., & Chen, X. (2020). Experimental investigation on startup process for oil supply system of a variable speed rotary compressor. International Journal of Refrigeration, 113, 58-69.
17. Arqam, M., Dao, D. V., Mitchell, M., & Woodfield, P. (2021). Transient start-up of an electric swashplate refrigeration compressor. *Applied Thermal Engineering*, 196, 117351.
18. Zou, H., Li, X., Tang, M., & Tian, C. (2021). Start-up Characteristics of Linear Compressors in a Refrigeration System. *Journal of Thermal Science*, 30(2), 598-609.